

Montclair State University

## Montclair State University Digital Commons

---

Department of Earth and Environmental Studies Faculty Scholarship and Creative Works Department of Earth and Environmental Studies

---

2020


### Environmental Forensics of Complexly Contaminated Sites: A Complimentary Fingerprinting Approach

Michael A. Kruge  
krugem@mail.montclair.edu

Azucena Lara-Gonzalo  
*University of Oviedo*

José Luis Gallego  
*University of Oviedo*

Follow this and additional works at: <https://digitalcommons.montclair.edu/earth-environ-studies-facpubs>

 Part of the [Analytical Chemistry Commons](#), [Earth Sciences Commons](#), and the [Environmental Sciences Commons](#)

---

#### MSU Digital Commons Citation

Kruge, Michael A.; Lara-Gonzalo, Azucena; and Gallego, José Luis, "Environmental Forensics of Complexly Contaminated Sites: A Complimentary Fingerprinting Approach" (2020). *Department of Earth and Environmental Studies Faculty Scholarship and Creative Works*. 62.  
<https://digitalcommons.montclair.edu/earth-environ-studies-facpubs/62>

This Article is brought to you for free and open access by the Department of Earth and Environmental Studies at Montclair State University Digital Commons. It has been accepted for inclusion in Department of Earth and Environmental Studies Faculty Scholarship and Creative Works by an authorized administrator of Montclair State University Digital Commons. For more information, please contact [digitalcommons@montclair.edu](mailto:digitalcommons@montclair.edu).

## PREPRINT

Michael A. Kruge, Azucena Lara-Gonzalo, José Luis R. Gallego,  
Environmental forensics of complexly contaminated sites: A complimentary fingerprinting approach,  
Environmental Pollution, Volume 263, Part B, 2020, 114645, ISSN 0269-7491,  
<https://doi.org/10.1016/j.envpol.2020.114645>.  
(<http://www.sciencedirect.com/science/article/pii/S0269749119370307>)

Environmental Forensics of Complexly Contaminated Sites:

A Complimentary Fingerprinting Approach

Michael A. Kruge<sup>a\*</sup>, Azucena Lara-Gonzalo<sup>b</sup>, José Luis R. Gallego<sup>c</sup>

<sup>a</sup>Department of Earth & Environmental Studies, Montclair State University, Montclair, NJ  
07043, USA

<sup>b</sup>Environmental Assays Unit, Scientific and Technical Services (SCTs), Campus de Mieres,  
University of Oviedo, C/Gonzalo Gutiérrez Quirós. S/N, 33600 Mieres (Asturias), Spain

<sup>c</sup>INDUROT and Environmental Technology, Biotechnology and Geochemistry Group,  
Campus de Mieres, University of Oviedo, C/Gonzalo Gutiérrez Quirós. S/N, 33600 Mieres  
(Asturias), Spain

\*Corresponding author. ([krugem@montclair.edu](mailto:krugem@montclair.edu))

Abstract

The environmental forensics approach is most often applied in petroleum and fuel spill incidents, for which sophisticated chemical fingerprinting procedures have evolved. In cases in which pollutant discharges occur in settings with prior contamination, more care must be taken in source discrimination, requiring further advances in methodology.

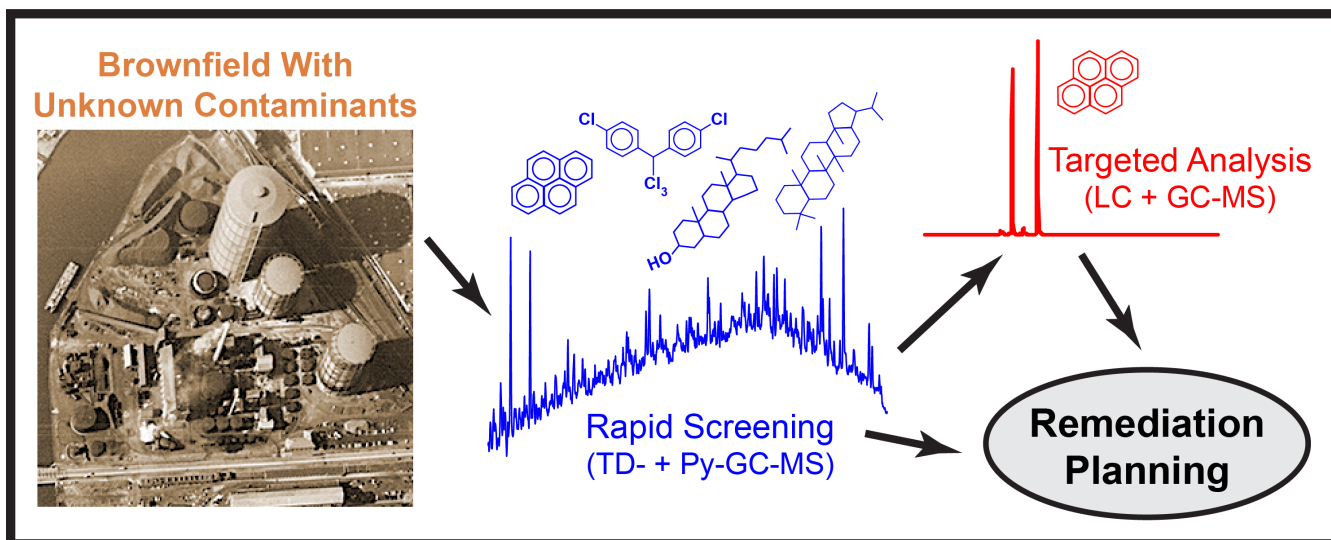
Additional obstacles can arise if the spill is an atypical industrial discharge. This would necessitate painstaking characterization of unfamiliar substances lying outside of existing regulatory regimes and thus overlooked by mandated analytical protocols (i.e., contaminants

of emerging concern). Towards these ends, this paper presents a systematic, multi-faceted GC-MS approach using the saturated, aromatic, and resin fractions of contaminated soil extracts, alongside soil thermal desorption and analytical pyrolysis of the soil and its asphaltene fraction. This complimentary "extract + thermal" approach is applied to a typical fuel oil spill, sediments of a severely-impacted urban river, and brownfield soils from coke, petrochemical, and Hg-As pyrometallurgical plants. The insights thus attained can serve to better inform brownfield remediation planning in the public interest.

### Highlights

- Environmental forensic methods for brownfields with complex contamination histories
- Characterization of unfamiliar pollutants lying outside of existing regulatory regimes
- Multi-faceted GC-MS approach using all SARA fractions including asphaltenes
- Pyrolysis-GC-MS providing effective, rapid soil contaminant assessment

Keywords: Soil pollution; post-industrial brownfields; environmental forensics; chemical fingerprinting; pyrolysis-GC-MS



Graphical Abstract

## 1. Introduction

Since the last century, a large number of compounds have been designated as possible environmental contaminants. Comprehensive monitoring of these substances is crucial to protect soil quality, but also to address their sources and fate, together termed the environmental forensics approach. In environmental forensics investigations, it is very useful to adopt non-targeted methods, which can screen for the presence of a large number of contaminants, rather than focusing on only a limited number of analytes (Douglas et al., 2007) or a mere quantification of usual parameters. In fact, concurrent contamination of complex chemicals affecting soil, subsoil and sediments poses a challenging problem for site remediation (Lara-Gonzalo et al., 2015). In this sense, a forensic approach requires different methodologies in order to fingerprint distinctive features of site- or source-specific contamination.

Fingerprinting methodologies have been mainly developed as tools in the environmental assessment of hydrocarbon pollution (Boehm et al., 1997; Medeiros and Simoneit, 2007; Uhler et al., 2010; Balseiro-Romero et al., 2016; Rosell-Melé et al., 2018; Stout et al., 2018). The principal objectives of these techniques are: (a) to characterize the type of fuel causing the contamination, (b) to quantify the concentration of compounds potentially hazardous to the environment, (c) to investigate the degree of chemical and biological degradation of contaminants, and (d) to determine their source, fate and transport in the environment using the compositional patterns of fuel contaminants (Alimi et al., 2003). In addition, these techniques can be used in other types of samples to achieve the same objectives, such as industrial releases (Thavamani et al., 2011; Lara-Gonzalo et al., 2015).

Gas chromatography-mass spectrometry (GC-MS) techniques have been shown to be powerful tools for environmental studies and chemical fingerprinting (Boehm et al., 1997; Krüge and Permanyer, 2004; Medeiros and Simoneit, 2007; Wait and Ramsey., 2007; Uhler

et al., 2010; Balseiro-Romero et al., 2016; Rosell-Melé et al., 2018). In the case of complex mixtures of pollutants, the liquid chromatographic (LC) fractionation prior to the GC-MS analysis of the fractions helps to unravel the heterogeneous information resulting from multiple or very complex pollution sources. Moreover, the application of single-shot or double-shot pyrolysis-gas chromatography-mass spectrometry (Py-GC-MS) additionally offers another forensic approach, particularly for unconventional mixtures (Lara-Gonzalo et al., 2015; Kruge, 2015; Kruge et al., 2018; Haggmann et al., 2019). Specifically, the double-shot Py-GC-MS consists of a two-step analysis. In the first step, thermodesorption performed at lower temperatures (e.g. 350°C), the volatile and semivolatile materials are released from the sample. Subsequently, the remaining sample residue is heated at a higher pyrolysis temperature to evolve the true pyrolysis products (Krugue, 2015; Krugue et al., 2018).

Following the preceding considerations, the contamination in the diverse soil and sediment samples examined in this work originated as very different types of industrial releases. Two different, but complementary, approaches were taken. Firstly, a “classical” extraction approach involving LC fractionation followed by GC-MS of maltene fractions along with Py-GC-MS of asphaltenes, and the second a “non-extraction” double-shot approach by means of thermodesorption (TD-GC-MS) for semivolatiles, followed by pyrolysis (Py-GC-MS) of the thermodesorption residue. (NB: When the raw extract is taken up in excess light *n*-alkane solvent (e.g., *n*-hexane), the heavy *asphaltenes* precipitate and are removed, while the remaining components (termed *maltenes*) go into solution, ready for subsequent LC fractionation, as described in Sec. 2.) The data are interpreted in the context of the samples’ diverse origins, emplacement and weathering using an environmental forensics approach. In addition, insights from the thermodesorption and pyrolysis methods are presented, including an evaluation of their effectiveness as forensic screening tools. We

hypothesized that the second approach may enhance and support the information obtained with common GC-MS fingerprinting methods.

## 2. Materials and methods

### 2.1. Samples

Five soil and sediment samples from different brownfield sites were studied. The first two represent many typical spill/releases in the industrial sites, i.e. a fuel spill and coal tar residues, a third one constitutes a complex, multi-contaminant record in urban fluvial sediment, and the last two are associated with non-conventional or more specific releases/waste disposal respectively linked to the petrochemical industry and non-ferrous metallurgy. The main issues about the five individual sites and samples are detailed in Section 2.2.1.

### 2.2. Experimental Methods

#### 2.2.1. Sample Preparation

Sample F is tar (heavy fuel oil) that was collected in a former industrial site within the context of the LIFE I+DARTS project (Gallego et al., 2015). It was taken in the western area of the El Terronal site (NW Spain), at a former As-Hg mining-metallurgy complex that has been subjected to intense weathering and biodegradation after more than 45 years of abandonment, with no environmental remediation to date (Gallego et al., 2015). The sample (pure product) was obtained in an untreated soil affected by a sub-surface heavy fuel spill from a underground storage tank. It was stored in glass and preserved in darkness at 4 °C until analysis.

Sample C is a soil taken in the surroundings of a former coke oven unit (García et al., 2012). In this sort of installation, the typical pollutants include coal tar and related compounds. It was obtained in 2012 from a characterization campaign done in the soil affected by this semi-industrial coking plant (with more than 30 years of operation) located near Oviedo (northern Spain). That study was focused on the evaluation of emissions and releases associated with coal, coke and sub-products handling and the coking process (García et al., 2012). The sample (composite) was taken just after the closure of the coking plant from a depth up to 10 cm in the surroundings of the coke ovens. It was stored in glass and preserved in darkness at 4 °C, and prior to analysis it was dried at 40 °C.

Sample R was taken from a sediment core collected for a United States Environmental Protection Agency (USEPA) study of contamination in the estuarine Passaic River, New Jersey, USA, as part of the Lower Passaic River Restoration Project including the Diamond Alkali Superfund site (Malcolm Pirnie, Inc., 2006; USEPA, 2019). It is from a slice (131-140 cm sediment depth) of core 17D taken in 2005 in a heavily urbanized and historically industrial reach of the Passaic River between Newark and Harrison, NJ (40.739029 °N, 74.142866 °W). The fresh core had been divided into sequential, homogenized sub-samples (“slices”), aliquots of which had been stored in glass jars while still wet and then frozen. The Passaic River Institute at Montclair State University received these samples in the frozen state from the USEPA contractor. The sample for this study was thawed, dried overnight in a Fisher Scientific Isotemp oven at 35 °C, and disaggregated by hand using a mortar and pestle, appearing fine-grained and medium gray in color at the end of the procedure.

Sample P (from an unpublished location in southern Europe) was taken in 2014 in soil surrounding a former petrochemical unit that primarily produced styrene. The plant employed the styrene monomer propylene oxide (SMPO) process for decades and it was



closed by 2010. The sample (composite) was taken in area where a previous screening indicated severe pollution and consist of several increments taken up to 30 cm depth. It was stored in glass and preserved in darkness at 4 °C; prior to analysis it was dried at 40 °C.

Finally, Sample M is a blend of soil and a metallurgical waste located in a former Hg-As pyrometallurgical plant, taken in the same polluted area as sample F (González-Fernández et al., 2018). It consist of some aggregates of natural soil mixed with a metallurgical waste denominated stupp (Gallego et al., 2015) which is a dark residue (soot and ore dust) from the processing of mercury ore, specifically from the Hg condensing system. The sample was taken in the vicinity of stupp stock-piles and it was storage in glass and preserved in darkness at 4 °C; prior to analysis it was dried at room temperature to avoid Hg volatilization.

### 2.2.2. Extraction and LC Fractionation

Measured amounts of the soil samples (5 to 10 g) were extracted with dichloromethane:methanol (3:1, v/v) in a Soxtherm system (C. Gerhardt GmbH, Königswinter, Germany) at 150 °C for 3 h. The extracts were concentrated by rotary evaporation and aliquots were fractionated and gravimetrically quantified by deasphalting and liquid chromatography (LC) into four fractions. In brief, maltenes and asphaltenes were separated by filtering through 0.45 µm PTFE filters, first using *n*-hexane to remove the maltenes, followed by dichloromethane to mobilize the asphaltenes. Then, the maltenes were separated into three fractions from lesser to greater polarity in an LC column (Corning 7078-5N serological disposable glass pipette) filled with activated (dried overnight at 240 °C) silica gel (4/5) and alumina (1/5). Fraction 1 (saturates) was eluted with hexane, fraction 2 (aromatics) with dichloromethane:hexane (7:3, v/v), and finally, fraction 3 (resins) with dichloromethane:methanol (1:1, v/v) (Fig. 1). The desasphalting and LC methodologies evolved based upon published sources (ASTM, 2007; de la Cruz, 1997; Jewell et al., 1974;

USEPA, 1996). Blanks, duplicates, and representative standard materials (petroleum, fuel oil, etc.) were routinely used to monitor the performance of the analytical processes for quality control and assurance (QA/QC) purposes.

Figure 1

### 2.2.3. Conventional GC-MS

The analyses of the three maltene fractions were carried out by GC-MS (Fig. 1). The injection of the extracts was performed on a GCMS-QP2010 Plus (Shimadzu Europa GmbH, Duisburg, Germany). A DB-5MS capillary column (5% phenyl, 95% dimethylpolysiloxane; 60 m x 0.25 mm i.d. x 0.1  $\mu\text{m}$  film) from Agilent Technologies was used with helium as carrier gas at 1 mL  $\text{min}^{-1}$ . The initial oven temperature was 50  $^{\circ}\text{C}$  (held for 2 min) and ramped at 2.5  $^{\circ}\text{C min}^{-1}$  up to 310  $^{\circ}\text{C}$  and held for 45 min. The mass spectrometer was operated in electron ionization mode (EI) at 70 eV. It was calibrated daily by autotuning with perfluorotributylamine (PFTBA) and the chromatograms were acquired in full scan mode (mass range acquisition was performed from 45 to 500 m/z). For quality control, solvent blanks were periodically injected. Compounds were identified using the W8N08 mass spectral library (John Wiley and Sons, Inc., New York, NY), the NIST27 and NIST47 mass spectral libraries (chemdata.nist.gov), the online NIST Standard Reference Database Number 69 (webbook.nist.gov/chemistry/), and by reference to the literature (Krüge, 2015; Krüge et al., 2010; 2018; Lara-Gonzalo et al., 2015, and references therein).

### 2.2.4. Thermodesorption-GC-MS and Pyrolysis-GC-MS

TD-GC-MS and Py-GC-MS were accomplished using a CDS 5150 Pyroprobe (CDS Analytical Inc., Oxford, PA) coupled to a Thermo Finnigan Focus DSQ GC/MS (Thermo

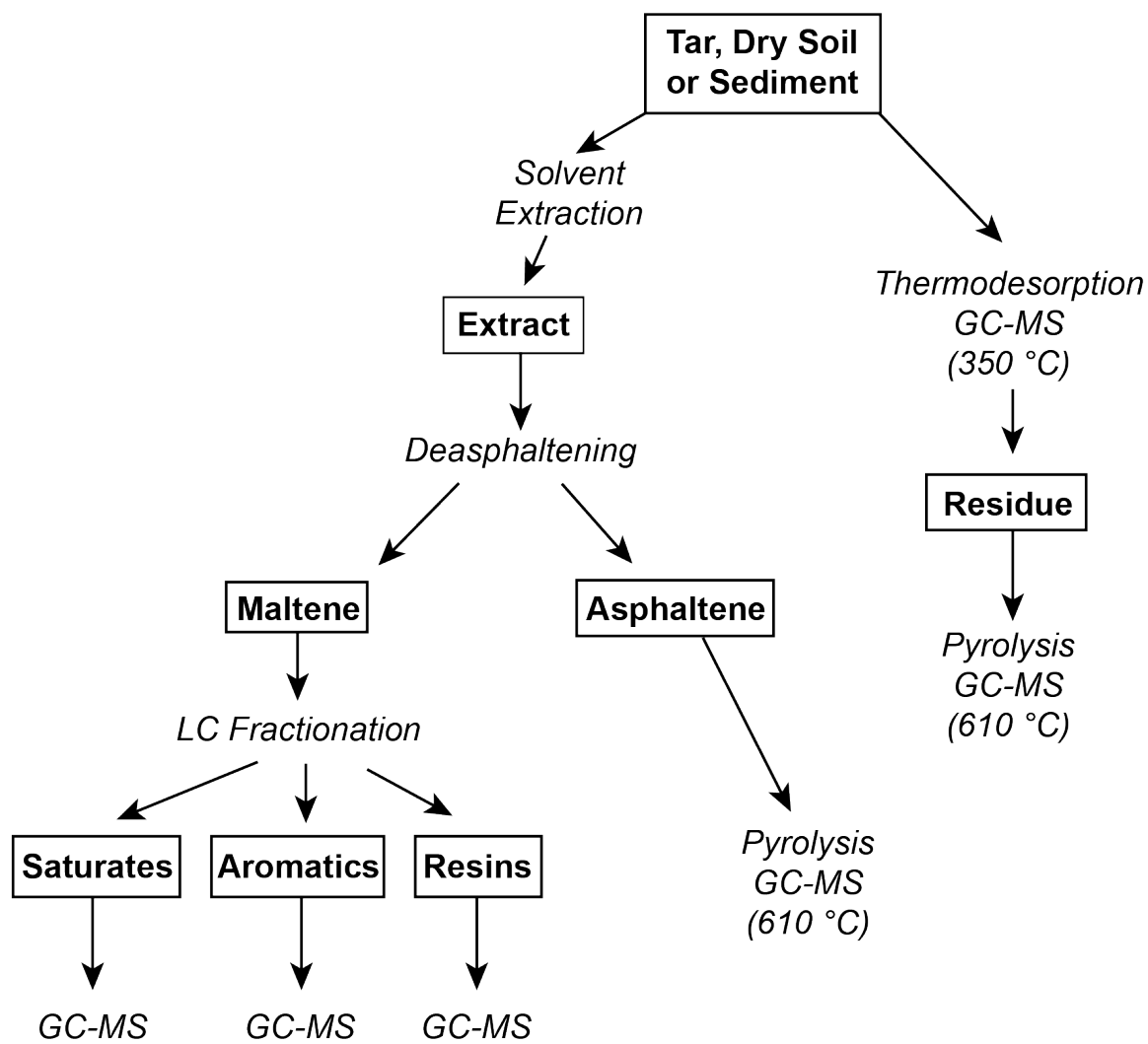


Figure 1. Flow chart illustrating the sequence of analytical procedures employed

Electron Corporation, Madison, WI) equipped with an Agilent DB-1MS column (30 m x 0.25 mm i.d. x 0.25  $\mu\text{m}$  film thickness). Thermodesorption was performed on a measured amount of dry soil or sediment (1 to 4 mg) for 20 s at 350 °C. In cases for which the initial amount was inadequate for optimal signal-to-noise or excessive, leading to column overloading, the sample quantity was adjusted and the analysis repeated. The GC oven temperature was programmed from 50 °C to 300 °C (at 5 °C  $\text{min}^{-1}$ ), with an initial hold of 5 minutes at 50 °C and a final hold of 15 minutes at 300 °C. The MS was operated in full scan mode (50-500 Da, 1.08 scans  $\text{s}^{-1}$ ). After the thermodesorption run ended, the sample (which had remained untouched in the Pyroprobe) was heated at 610 °C for 20 s, pyrolyzing the post-thermodesorption residue ("double-shot" or "sequential pyrolysis"). Pyrolysis products were analyzed by GC-MS (Py-GC-MS) using the conditions employed for the thermodesorption products. Using the same GC-MS conditions, Py-GC-MS (610 °C, 20 s) was performed directly on the asphaltene fractions (<0.1 mg), without the thermodesorption step (Fig. 1).

Unlike the others, Sample M was analyzed in a "single shot" (610 °C, 20 s) for a combined thermodesorption-pyrolysis. Asphaltenes from Sample R were not pyrolyzed. For quality assurance and quality control (QA/QC), the mass spectrometer was calibrated by autotuning with PFTBA. Daily blank runs were made prior to sample analysis. Even though this TD- and Py-GC-MS work is qualitative, selected sample analyses were repeated to monitor for consistency in the results. Compounds were identified as described in Section 2.2.3.

### 3. Results and Discussion

#### 3.1. Overview of General Characteristics

The five samples discussed in the work represent a variety of soils and sediments polluted by industrial releases. They are genetically unrelated and represent wide compositional variety as reflected in Table 1. Three of them were expected to correspond with some of the typical fingerprints found in many brownfield samples/sites; i.e. a fuel oil (F), coal-tar like (C), and mixed fossil fuel, sewage, and pesticide (R) fingerprints. In contrast, the other two (P and M) were anticipated to be atypical.

The fuel spill sample (F) was found to contain a slight predominance of aromatic hydrocarbons (36.7 %) with the balance being roughly similar amounts of saturated hydrocarbons, resins and asphaltenes (17-24%) (Table S1, Fig. S1). In contrast, the soil contaminated with coke oven residues (C) produced 9.32 g kg<sup>-1</sup> soil of extractable material, of which 84.1 % is asphaltenes. Its resin fraction is only 9.4%, while its saturate and aromatic hydrocarbons comprise a mere 2.9 and 3.6%, respectively. The urban river sediment (R) has a total soluble extract (TSE) yield of 8.46 g kg<sup>-1</sup> dry sediment, with a predominance of saturated hydrocarbons (39.8%) as well as abundant asphaltenes (26.9%). The petrochemical plant soil (P) yielded 9.33 mg kg<sup>-1</sup>, predominantly resins (47.5%) and asphaltenes (39.3%). Upon extraction, the waste and soil from the metallurgical plant (M) produced 5.06 g kg<sup>-1</sup> which, like sample C, is predominantly asphaltenes (85.5%) with 9.9% resins (Table S1, Fig. S1).

## 3.2. Molecular analyses

### 3.2.1. Sample F - Fuel spill

The saturated hydrocarbon fingerprint (Fig. 2A; peak identifications in Table 1) of the fuel spill (Sample F) displays a complete absence of *n*-alkanes or branched alkanes irrespective of chain length, whereas sesquiterpenes [peaks SQ<sub>n</sub> for which "n" is the carbon number], tricyclics [e.g., TR23], tetracyclic terpane [TT] and especially hopanes [H<sub>n</sub>, T<sub>s</sub>, T<sub>m</sub>] are relatively abundant. (Note that peak symbols are enclosed in square brackets). The UCM ("unresolved complex mixture") hump reflects the predominance of heavier compounds with a maximum eluting under the C<sub>29</sub> hopane [H29]. In addition, the TIC (total ion chromatogram) trace of the aromatics also exhibits a prominent UCM hump with a broad plateau (Fig. 2B). PAHs (polycyclic aromatic hydrocarbons) and alkyl-PAHs are clearly minor, whereas the predominant compounds are aromatic biomarkers including aromatic 8,14-secohopanoids [SH<sub>n</sub>] and benzohopanes [BH<sub>n</sub>] along with alkyldibenzothiophenes [DBT<sub>x</sub>, where "x" is the degree of alkylation for aromatic compounds]. Finally, in Fraction 3 (resins) only the presence of some steroids [STL29, STO29] is noticeable (Fig. 2C).

Figure 2

Table 1

Upon thermodesorption (Fig. 2D), the sample yielded mainly alkyldibenzothiophenes [DBT<sub>x</sub>] and hopanes [H<sub>n</sub>, T<sub>s</sub>, T<sub>m</sub>] consistent with those seen in the saturated and aromatic fractions (Fig. 2D), as well as a prominent UCM hump having a maximum again coincident with hopane peak H29. The residue after thermodesorption is predominantly aliphatic, as attested by the series of *n*-alkane/*n*-alk-1-ene doublets (numbered peaks in Fig. 2E), as is the

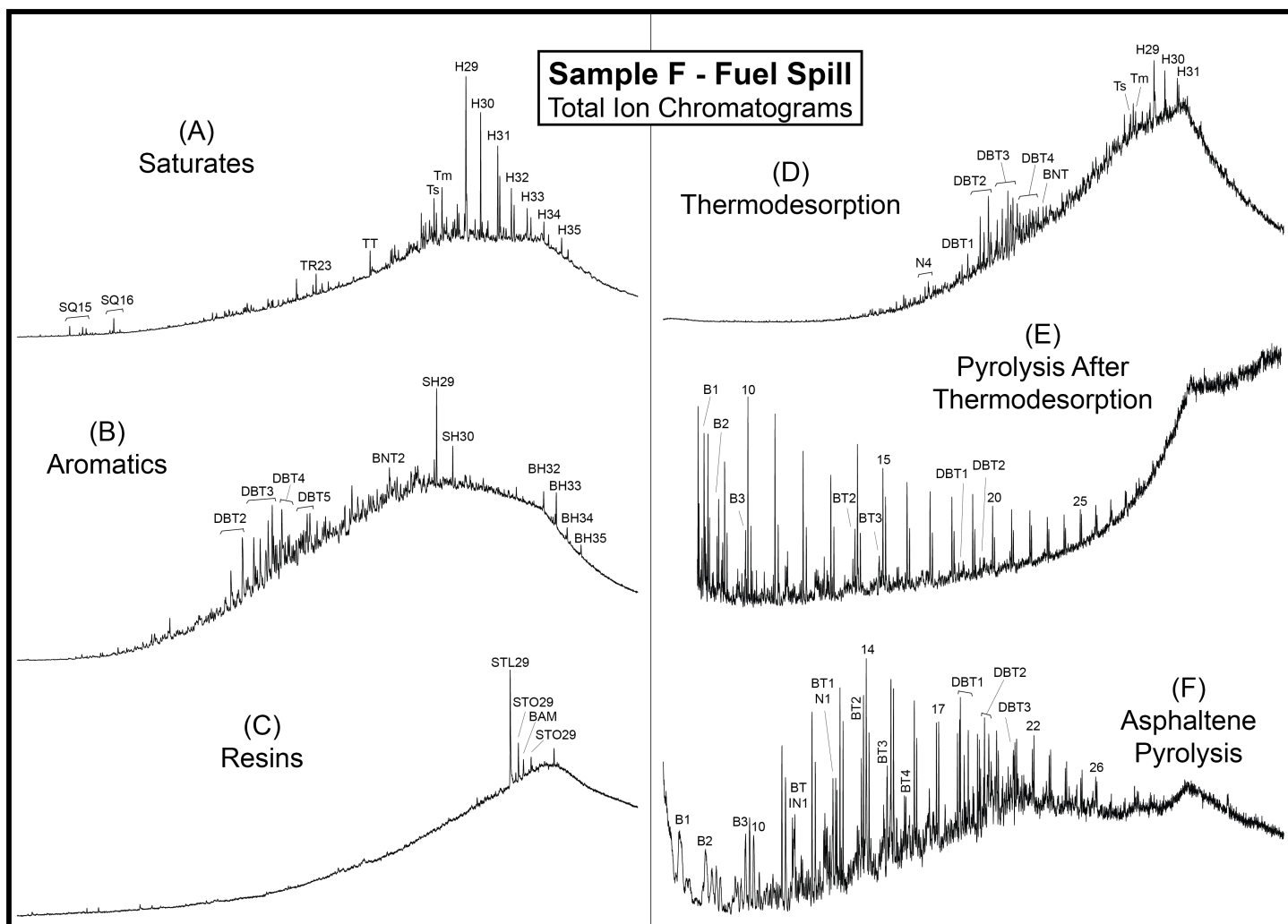


Figure 2. Total ion current chromatograms for fuel spill Sample F. (A) saturated hydrocarbons, (B) aromatics, (C) resins, (D) thermodesorption products, (E) products of sequential pyrolysis of the post-thermodesorption residue and (F) asphaltene pyrolysis products. See Table 1 for peak identification.

Symbol	Component	Type	Symbol	Component	Type
numerals	normal alkanes ( <i>n</i> -alk-1-ene/ <i>n</i> -alkane doublets for pyrolyzates)	ALIPH	FLU	fluorene	AROM
ABT	abietane derivatives	AROM	FLU <sub>x</sub>	alkylfluorene isomers	AROM
ACE	acenaphthalene	AROM	Fon	phenolethanone	OXYG
ACP	cyclopenta[ <i>cd</i> ]pyrene isomer	AROM	Fr	farnesane	ALIPH
ACR	acridine	NITRO	HF	homofarnesane	ALIPH
ACY	acenaphthylene	AROM	Hg	elemental mercury	INORG
AMn	alkylamides ("n" indicates the carbon number)	NITRO	Hn	hopanes ("n" indicates the carbon number, C29-C35)	ALIPH
ANT	anthracene	AROM	IN <sub>x</sub>	alkylindene isomers	AROM
ANTO	anthracene-dione isomer	OXYG	IPYR	indeno[1,2,3- <i>cd</i> ]pyrene	AROM
ANTO1	methylanthracene-dione isomer	OXYG	LBD	labdadienol isomer (diterpenoid)	OXYG
As4O6	arsenolite	INORG	N	naphthalene	AROM
B	benzene	AROM	N <sub>x</sub>	alkylnaphthalene isomers	AROM
B <sub>x</sub>	alkylbenzene isomers	AROM	NP	norpristane	ALIPH
BACR	benzoacridine isomer	NITRO	OLn	alkanols ("n" indicates the carbon number)	OXYG
BAM	beta-amyrin or similar pentacyclic triterpenoid	OXYG	Ph	phytane	ALIPH
BAN	benzo[ <i>a</i> ]anthracene	AROM	PHN	phenanthrene	AROM
BANCN	benzo[ <i>a</i> ]anthracene carbonitrile isomer	NITRO	PHN <sub>x</sub>	alkylphenanthrene and alkylanthracene isomers	AROM
BCBZ	benzocarbazole	NITRO	PHNF	phenanthrofurans isomers	OXYG
BCP	benzo[ <i>c</i> ]phenanthrene (?)	AROM	PNAP	phenylnaphthalene isomers	AROM
BFLA	benzofluoranthenes	AROM	Pr	pristane	ALIPH
BFLU	benzofluorene isomers	AROM	PYR	pyrene	AROM
BFO	benzofluorenone	OXYG	PYR <sub>x</sub>	alkylpyrene and/or alkylfluoranthene isomers	AROM
BHn	benzohopanes ("n" indicates the carbon number)	AROM	RET	retene	AROM
BNF	benzophthofuran	OXYG	RETHH	retene, tetrahydro	AROM
BNT	benzophthothiophene	SULF	S8	elemental sulfur	SULF
BNT <sub>x</sub>	alkylbenzophthothiophene isomers	SULF	SHn	aromatic 8,14-secohopanooids ("n" indicates the carbon number)	AROM
BPER	benzo[ <i>ghi</i> ]perylene	AROM	SQn	sesquiterpanes ("n" indicates the carbon number)	ALIPH
BPYR	benzopyrenes	AROM	St	styrene	AROM
BPYR <sub>x</sub>	alkylbenzopyrene isomers	AROM	St <sub>x</sub>	alkylstyrene isomer	AROM
BT	benzothiophene	SULF	STEn	sterenes ("n" indicates the carbon number)	ALIPH
BT <sub>x</sub>	alkylbenzothiophene isomers	SULF	STLn	stanols & sterols ("n" indicates the carbon number)	OXYG
CBZ	carbazole	NITRO	STn	steranes ("n" indicates the carbon number)	ALIPH
CH2C12	dichloromethane	CHLOR	STOn	stanones & stenones ("n" indicates the carbon number)	OXYG
CHR	chrysene	AROM	Tm	17 $\alpha$ (H)-22,29,30-trisnorhopane	ALIPH
CHR <sub>x</sub>	alkylchrysene & alkylbenzo[ <i>a</i> ]anthracene isomers	AROM	TRn	tricyclic terpanes ("n" indicates the carbon number)	ALIPH
DBA	dibenzoanthracene isomers	AROM	Ts	18 $\alpha$ (H)-22,29,30-trisnorhopane	ALIPH
DBF	dibenzofuran	OXYG	TT	C24 tetracyclic terpane	ALIPH
DBPYR	dibenzopyrenes	AROM	X	plasticizers (phthalates and TXIB)	OXYG
DBT	dibenzothiophene	SULF	●●	biphenyl	AROM
DBT <sub>x</sub>	alkyldibenzothiophene isomers	SULF	●●●	terphenyl	AROM
DCn	alkyldecalin ("n" indicates the carbon number)	ALIPH	●●○	biphenylcyclohexane	AROM
DDC	bis(cholorophenyl)ethane, chloro	CHLOR	●○	phenyldicyclohexane	AROM
DDD	bis(cholorophenyl)ethane, dichloro	CHLOR	○○	tricyclohexane	ALIPH
DDE	bis(cholorophenyl)ethene, dichloro	CHLOR	●●●	quaterphenyl	AROM
DDM	bis(cholorophenyl)methane	CHLOR	●●○	terphenylcyclohexane	AROM
DDO	bis(cholorophenyl)ethanone	CHLOR	●●○	diphenyldicyclohexane	AROM
DDT	bis(cholorophenyl)ethane, trichloro	CHLOR	●○○	phenyltricyclohexane	AROM
DOE	dioctyl ether	OXYG	●●●●	quinquephenyl	AROM
DSn	diasteranes ("n" indicates the carbon number)	ALIPH	●●●○	quaterphenylcyclohexane	AROM
F	phenol	OXYG	●●○○	terphenyldicyclohexane	AROM
F <sub>x</sub>	alkylphenol isomers	OXYG	●●●○	quinquephenylcyclohexane	AROM
FCA	furfural	OXYG		numeral with polyphenyl symbol indicates degree of alkylation	
FLA	fluoranthene	AROM		polyphenyl symbol with -O or -N: oxygen or nitrogen substitution	

Table 1. Peak identification. Aliphatic hydrocarbons (ALIPH), aromatic hydrocarbons (AROM), sulfur compounds (SULF), oxygenated compounds (OXYG), organonitrogen compounds (NITRO), organochlorine compounds (CHLOR), inorganic components (INORG). For alkyl-substituted aromatic hydrocarbons and heterocompounds, x indicates the degree of substitution. (1: methyl, 2: dimethyl or ethyl, etc.).



asphaltene pyrolyzate (Fig. 2F), although the latter appears more aromatic and sulfur-rich, with a pronounced UCM hump. In contrast to the extract fractions and thermally-desorbed products (Fig. 2A-D), the pyrolyzates contain proportionally more lower molecular weight aromatic hydrocarbon [Bx] and sulfur [BTx] compounds (Fig. 2E, F).

This sample exhibits severe biodegradation of 4-6 on the Peters et al. (2005) scale suggesting an intense weathering, consistent with the age (more than 40 years) of the spill. The bias towards higher molecular weight components in the extracted and thermally-desorbed materials reflects the heavy nature of the original fuel spill, evidently also sulfur-rich (Figs. 2A-D, Table 2). Even though biodegradation has eliminated the *n*-alkanes in the extract (Fig. 2A), they appear to have been regenerated or released from asphaltenes during pyrolysis (Fig. 2E, F), a phenomenon previously noted (Kruge et al., 2018). Their presence attests that the sample is indeed a petroleum product, dating from an earlier era prior to restrictions on fuel sulfur content.

Table 2

### 3.2.2. Sample C - Coke oven soil

The TIC trace of Sample C's saturated hydrocarbon fraction exhibits *n*-alkanes from C<sub>14</sub> to at least C<sub>30</sub> with a maximum at C<sub>23</sub>, isoprenoids (Pr >> Ph), C<sub>29</sub>-C<sub>35</sub> hopanes, elemental sulfur [S8], and a prominent UCM hump in the *n*-C<sub>23</sub> to C<sub>40</sub> retention time range (Fig. 3A). The aromatic fraction shows parent PAHs [PHN, PYR, CHR] predominant over C<sub>1</sub> or C<sub>2</sub>-alkylated PAHs [PHNx, PYR1, CHR1], phenylnaphthalene [PNAP], along with aromatic oxygen and sulfur compounds such as dibenzofuran [DBF], benzonaphthofuran [BNF] and benzonaphthothiophene [BNT] (Fig. 3B). Unexpectedly, and surely as an artifact of the LC process employed, heavy aromatic compounds such as benzofluoranthenes,

Sample	Source	Main features identified		Comments
		"Extraction approach"	"Thermal approach"	
F	<i>Tar from biodegraded heavy fuel spill</i>	UCM, hopanoids & dibenzothiophenes prominent in SAT & ARO; <i>n</i> -alkanes & isoprenoids absent.	UCM, hopanoids & dibenzothiophenes prominent in TD; light aliphatics, aromatics, and sulfur compounds released in PYRO & ASPH.	Severely biodegraded, 40 year old spill of heavy, sulfur-rich fuel oil.
C	<i>Soil affected by releases from coke battery operations</i>	<i>n</i> -Alkanes and isoprenoids (Pr >> Ph) coexisting with UCM (SAT); in ARO parent PAHs predominate with DBF & BNF; heavy 4- to 6-ring PAHs in RES.	Parent PAHs (TD); 1- to 5-ring parent & alkyl aromatics and phenols (PYRO); heavy PAHs (ASPH).	Coal tar and distillate are principal contaminants, biodegraded; raw coal particles likely also present (SAT, PYRO). Preparative methods developed for oil spills overwhelmed in this case.
R	<i>Mid 20th century urban river sediment affected by diverse sources</i>	UCM, isoprenoids, petroleum biomarkers, odd carbon number <i>n</i> -alkanes (SAT), parent & alkyl PAHs, retene, DDT, PCBs (ARO), sewage steroids, phthalates (RES)	UCM, isoprenoids, petroleum biomarkers, odd carbon number <i>n</i> -alkanes, parent & alkyl PAHs, DDT (TD), light aromatics and aliphatics (PYRO).	Complexly contaminated sediment: Biodegraded petroleum/fuel oil, coal tar, combustion airfall (fossil fuel & wood smoke), sewage, pesticides, PCBs. Also natural vegetation input.
P	<i>Soil affected by releases from petrochemical plant that produced styrene</i>	Tricyclohexane derivatives & minor petroleum markers (SAT); complex mix of 2- to 5-ring polyphenyls, alkylbenzenes, alkylstyrenes (ARO); oxygenated 2- to 5-ring polyphenyls (RES).	2- to 4-ring polyphenyls, alkylbenzenes, styrene, methylstyrene (TD, PYRO, ASPH); styrene monomer more abundant in PYRO & ASPH.	Soil impacted by styrene oligomers (discharged process by-products); also minor petroleum contamination.
M	<i>Soil mixed with Hg-As metallurgical waste</i>	UCM, isoprenoids, hopanes, odd carbon number <i>n</i> -alkanes (SAT); predominantly 2- to 4-ring parent PAHs (ARO); octadecanol, docosenamide, and minor modern plant biomarkers (RES).	Arsenolite and elemental Hg in PYRO but organics not detected; arsenolite confirmed by SEM & EDS; Hg present in ASPH with only traces of organics detected.	Mix of fuel oil, pyrogenic PAHs, and As & Hg phases from ore processing kiln and adjacent soil; Py-GC-MS detected inorganics, but not organics. Also natural vegetation input.

Table 2. Summary. SAT - saturated hydrocarbon fraction, ARO - aromatic hydrocarbon fraction, RES - resin fraction, TD - thermodesorption products, PYRO - post-thermodesorption pyrolysis products, ASPH - asphaltene pyrolysis products. For other abbreviations, see text and Table 1.

indeno[1,2,3-*cd*]pyrene, benzo[*ghi*]perylene and dibenzopyrenes [BFLA, IPYR, BPER, DBPYR] eluted in the resin fraction (Fig. 3C). The most characteristic compounds in this fraction are the O and N-compounds as benzofluorenone, benzoacridine and benzo[*a*]anthracene carbonitrile [BFO, BACR, BANCN].

### Figure 3

The thermally-desorbed products are almost exclusively aromatic (Fig. 3D). Toluene [B1] is relatively most abundant, followed by naphthalene [N], 2-methylnaphthalene [N1], biphenyl [●●], and acenaphthylene [ACY]. Parent PACs (polycyclic aromatic compounds in general including non-hydrocarbons) important in the aromatic fraction are also detected here, including phenanthrene, fluoranthene, pyrene, dibenzofuran, a cyclopenta[*cd*]pyrene isomer, chrysene, and several pentaromatics. Dichloromethane is also a noteworthy component. The thermodesorption residue's pyrolyzate contains a complex mixture of mono- to pentaaromatic hydrocarbons, parent as well as alkylated (Fig. 3E). Toluene [B1] and methylnaphthalenes [N1] are among the most abundant. Oxygenated aromatic compounds, particularly alkylphenols [Fx] and dibenzofuran [DBF], are also significant constituents. Aliphatic hydrocarbons such as *n*-tridecane [13] are present in relatively low abundance. The asphaltene pyrolyzate is strongly biased towards the heavy (4- to 6-ring) PAHs [CHR, BAN, BFLA, BPYR, IPYR, BPER] (Fig. 3F).

The co-occurrence of the UCM hump with a well-defined series of normal alkanes in the saturated fraction (Fig. 3A) evokes the image of a moderately biodegraded fuel, or alternatively, a mixture of biodegraded hydrocarbons with fresher material, the latter appearing like a coal tar distillate (Emsbo-Mattingly and Stout, 2011). It is likely that spilled material continually accumulated over the 30 years of the plant's operations, gradually

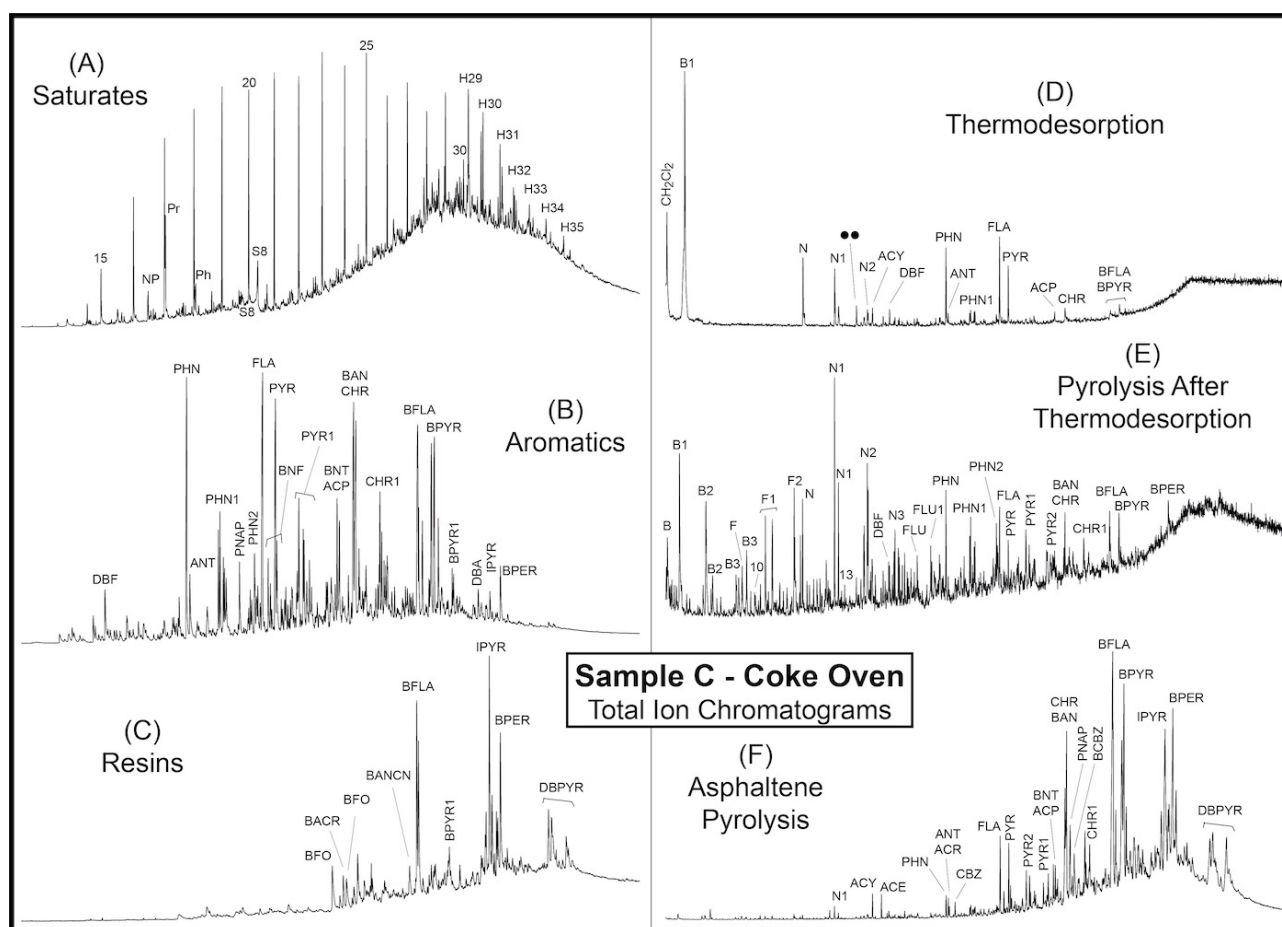


Figure 3. Total ion current chromatograms for coke oven soil Sample C. (A) saturated hydrocarbons, (B) aromatics, (C) resins, (D) thermodesorption products, (E) products of sequential pyrolysis of the post-thermodesorption residue and (F) asphaltene pyrolysis products. See Table 1 for peak identification.

degrading, with some relatively fresh material still present when the sample was taken shortly after the plant was closed (Sec. 2.2.1). With parent compounds predominating over the alkylated PAHs and the presence of dibenzofuran, Figures 3B and 3C taken together present the characteristic signature of a coal tar (Nishioka et al., 1986; Schobert and Song, 2002; Uhler and Emsbo-Mattingly, 2006; Emsbo-Mattingly and Stout, 2011). Thermodesorption products of spilled fuel in this study (Fig. 2) and previously reported (Kruege et al., 2018) appear as blends of the saturated and aromatic fractions. In contrast, Sample C's thermodesorption trace displays a limited number of parent PAHs, yet still presenting a coal tar fingerprint. Since the saturated and aromatic fractions represent only a small fraction of the extract (about 3 % each, Table S1), the thermodesorption trace likely represents a more synoptic picture of the sample since it was acquired directly from the whole soil. Thermally desorbed products from soils are typically limited to semi-volatile compounds (e.g., Fig. 3D). Volatile compounds like dichloromethane and toluene [ $\text{CH}_2\text{Cl}_2$ , B1] are not expected (Fig. 3D) and we speculate that they are perhaps solvents that were utilized as part of the coke plant operations and remained sequestered in the soil, perhaps adsorbed to particles of spilled coal.

The post-thermodesorption residue pyrolyzate (Fig. 3E) resembles that of a bituminous coal, with alkylated benzenes, phenols, naphthalenes, and PAHs predominating (Hatcher et al., 1992; Kruege & Bensley, 1994; Stankiewicz et al., 1994a; 1994b; Laumann et al., 2011), likely reflecting coal feedstock employed in the coke production spilled onto the soil. The *n*-alkanes in the saturate fraction (Fig. 3A) could thus have been extracted from the coal particles, in which they would have remained impervious to biodegradation. Asphaltene pyrolyzates in spilled fuel studies tend to resemble those of the post-thermodesorption residue, as seen in the present (Fig. 2E, F) and prior studies (Kruege et al., 2018), logical since asphaltenes present in the sample are too heavy to volatilize in response to the

thermodesorption conditions employed. However, in this case the asphaltene yielded a mixture of heavy PAHs closely resembling those in the resin fraction (Fig. 3C, F), in effect, a high-temperature volatilization of large, intact hydrocarbons rather than true pyrolytic cracking of macromolecules. Sample C's resin fraction was shown to in fact contain predominantly heavy PAHs. The preparative methods employed in this study for deasphalting and LC (Sec. 2.2.2) were designed and calibrated for oil spill studies but have been overwhelmed by this sample. When working with spill samples not suspected to be petroleum, caution should be exercised in the choice and operation of the preparative methods. Fortunately, the resin fraction was also analyzed in this case; solely interpreting the PAH distribution as seen in the aromatic fraction would clearly have led to erroneous conclusions. The battery of complementary analyses employed herein (Fig. 3, Table 2) thoroughly and clearly characterized Sample C as coal tar, the main byproduct generated in the coal carbonization process.

### 3.2.3. Sample R - Urban river sediment

The total ion chromatogram of the saturated hydrocarbon fraction of the Passaic River core sediment (Sample R) shows a broad UCM hump, prominent isoprenoids [Fr, HF, NP, Pr, Ph] and hopanes [Ts, Tm, Hn]. Steranes and diasteranes [ST27, DS27, DS29] along with long-chain *n*-alkanes with an odd carbon-number predominance [numbered peaks] are minor features (Fig. 4A). The aromatic hydrocarbons show a predominance of parent 3 to 5-ring PAHs [PHN, FLA, PYR, BAN, CHR, BFLA, BPYR] with secondary amounts of alkylated PAHs [PHN1, PYR1, CHR1] including retene and a derivative [RET, RETH], along with minor alkylnaphthalenes [Nx] (Fig. 4B). Aromatic 8,14-secohopanoids and benzohopanes [SHn, BHn] are also in evidence, as are relative minor amounts of the pesticide dichlorodiphenyltrichloroethane [DDT] and its derivatives [DDC, DDD, DDE]. Several

polychlorinated biphenyl (PCB) congeners with 5 to 7 chlorines are present, but in relative concentrations that are too low to produce visible peaks on Fig. 4B. Upon viewing its diagnostic  $m/z$  320, 322 and 324 mass chromatograms, 2,3,7,8-tetrachlorodibenzo-*p*-dioxin ("dioxin") was not detected, leading to the conclusion that this compound is likely not present in the sample, based on analytical methodologies used in this study. The resin fraction is characterized by relatively abundant  $C_{27}$  and  $C_{29}$  stanols [STLn] including coprostanol as well as stanones [STOn], diterpenoids [LBD], triterpenoids [BAM], long-chain even carbon-number *n*-alkanols, and minor amounts of a DDT derivative [DDO] (Fig. 4C). As was the case with sample C (Sec. 3.2.2, Fig. 3C), heavy 5- and 6-ring PAHs [BFLA, BPYR, IPYR, BPER, DBPYR] unexpectedly eluted in this fraction. The plasticizers dibutylphthalate and bis(2-ethylhexyl)phthalate [X] are also important components.

#### Figure 4

The most striking feature of Sample R's thermodesorption chromatogram is its prominent UCM hump (Fig. 4D). Riding this crest are a number of distinct peaks corresponding to isoprenoids [HF, Pr, Ph], long-chain odd carbon number *n*-alkanes [25-33], hopanes [Hn], steranes [DS27, DS29, ST29], and sterenes [STE27, STE29]. Di- to pentaaromatic hydrocarbons are also relatively important [Nx, PHNx, PYRx, RET, BAN, CHR, BFLA, BPYR]. Minor amounts of DDT derivatives [DDM] are in evidence. The pyrogram of the thermodesorption residue reveals monoaromatic hydrocarbons [Bx], phenols [Fx], naphthalenes [Nx], and lesser amounts of 3- and 4-ring PAHs (Fig. 4E). Mid- to long-chain *n*-alkane/*n*-alk-1-ene doublets without odd carbon number preference [11-30] indicate a significant aliphatic component. Sample R's asphaltenes were not pyrolyzed.

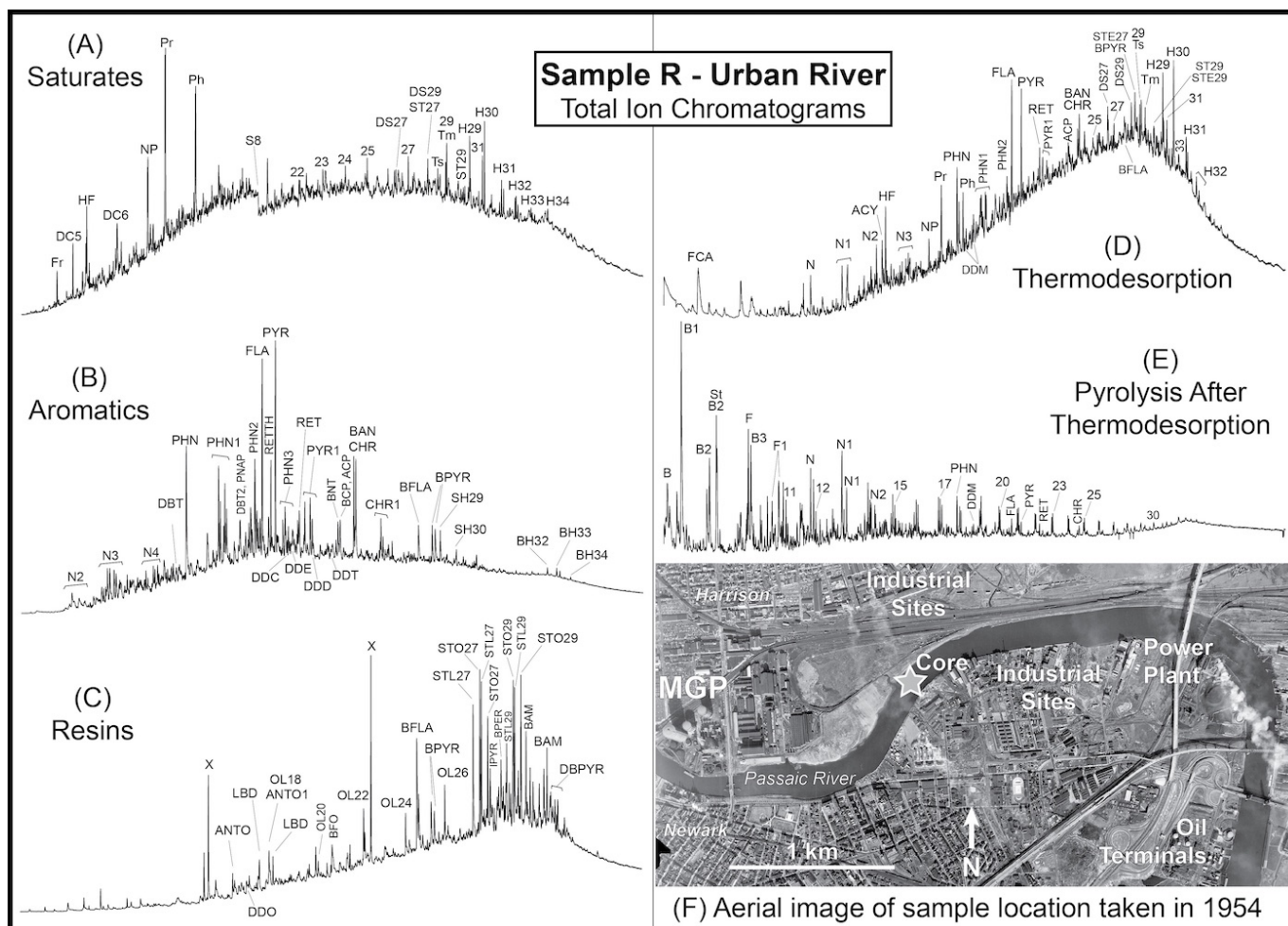


Figure 4. Total ion current chromatograms for urban river sediment Sample R. (A) saturated hydrocarbons, (B) aromatics, (C) resins, (D) thermodesorption products, (E) products of sequential pyrolysis of the post-thermodesorption residue. See Table 1 for peak identification. (F) Aerial image taken in 1954 of the sediment core location in the Passaic River between Newark and Harrison, New Jersey, approximately when the sediment was deposited. MGP: manufactured gas plant. Base image: United States Geological Survey archives ([earthexplorer.usgs.gov](http://earthexplorer.usgs.gov)). This sample's asphaltenes were not pyrolyzed.



The depth profile of publicly available  $^{137}\text{Cs}$  data for this core (USEPA-USACE, 2019) indicates a probable mid-20th century deposition for this sediment horizon, consistent with estimates of sedimentation rates in this reach of the river (Bopp et al., 1981, Malcolm Pirnie, Inc., 2006; Bujalski, 2010). The 1954 aerial image illustrates the urban density and multiple likely sources of sediment contamination of that time period, including a major manufactured gas plant (MGP), coal-fired power plant, petroleum terminals, and numerous industrial sites (Fig. 4F).

The isoprenoids, hopanoids, and UCM (Fig. 4A, B, D) all indicate an important contribution of biodegraded petroleum and/or heavy petroleum products to the contaminant mixture in this sediment (Boehm et al., 1997; Douglas et al., 2007). The long-chain, odd carbon number *n*-alkanes point to input from terrestrial vegetation in the watershed (Tissot and Welte, 1984). The PAH distribution, with parent compounds predominant yet with relatively abundant alkylated species (Fig. 4B, D), indicates a mix of both pyrogenic and petrogenic (Yunker et al., 2002). Point sources of combustion products are likely, given the visible smoke plumes in Fig. 4F, along with non-point sources in the watershed of which wood smoke is a factor, as attested by the presence of retene (Ramdahl, 1983; Simoneit, 2002; Bari et al., 2009). The observed PAHs are also consistent with contributions of coal tar constituents, most probably from the major MGP about 1 km upriver (Fig. 4F). With the presence of petroleum being well-documented by the saturated hydrocarbons, it is logical to assume that a portion of the observed alkyl-PAHs is similarly derived.

The  $\text{C}_{27}$  and  $\text{C}_{29}$  steroidal ketones and alcohols (including coprostanol) prominent in the resin fraction (Fig. 4C) attest to a third principal source of contamination to these sediments, namely raw or partially treated sewage (Grimalt et al., 1990; Mudge and Bebianno, 1997; Isobe et al., 2002). The storm sewer system in older cities, particularly in the northeastern USA like these, are linked to the sanitary sewers such that during a heavy

rainfall event, sewage overflows into waterways (Iannuzzi et al., 1995; 1997; Huntley et al., 1997). The C<sub>27</sub> and C<sub>29</sub> mono-unsaturated sterenes [STE27, STE29] in the thermodesorption products (Fig. 4D) are also sewage marker compounds, thermally altered to hydrocarbons during the analysis (Kruge et al., 2010). The phthalates detected in the resin fraction are also commonly present in historic Passaic River sewage outflows (Iannuzzi et al., 1997). The trace amounts of DDT and its derivatives detected (Fig. 4B-E) could be attributable to a manufacturing plant situated only about 500 m to the east, producing DDT since the 1940's (USEPA, 2019), although non-point sources cannot be excluded. Recall that with tidal mixing in this estuarine river, contaminant transport is both up- and downstream (Malcolm Pirnie, Inc., 2006). Beginning in the 1950's, this facility also manufactured the infamous defoliant Agent Orange employed during the Vietnam War, for which "dioxin" was a by-product that persists in sediments, now of great regulatory concern (Quadrini et al., 2015; USEPA, 2019). Thus the mid-20th century date estimated for the sediment layer appears reasonable, since DDT was detected, but "dioxin" was not (Bopp et al., 1981). The singularly complex, multi-contaminant mixture evident in the mid-20th century river sediment sample preserves the legacy of the location's industrial heyday, prior to the introduction of significant environmental protection legislation (Fig. 4, Table 2).

#### 3.2.4. Sample P - Petrochemical plant soil

Petrochemical plant soil Sample P differs markedly from those of the three previously presented contaminated sites. All six TIC traces (Fig. 5) show a strong predominance of polyphenyls, namely biphenyl [●●] and its 3- to 5-ring phenylogues with multiple isomers and degrees of alkyl substitution. Cyclohexyl rings replace aromatic ones in some instances. For peak identification a simple shorthand code is employed herein (Fig. 5, Table 1), for which a solid circle indicates a phenyl group [●] and an open circle, a cyclohexyl [○]. A

numeral represents the degree of alkylation, either between rings or as side substitutions, while -O and -N signal oxygen and nitrogen addition. Given the limitations of the mass spectral data and in the interest of brevity, little attempt is made to specify the isomers and thus Figure 5G presents a few possible structural examples (i-iii) consistent with the data.

Figure 5

The saturated hydrocarbon fraction (Fig. 5A) shows a predominance of saturated polyphenyl analogues including tricyclohexane [○○○] and phenyldicyclohexane [●○○] isomers, along with phenyltricyclohexane [●○○○] and relatively minor aliphatics, isoprenoids and hopanes. The aromatic hydrocarbon fractions (Fig. 5B) exhibits an extremely complex distribution of polyphenyl species ranging from biphenyl [●●] to quinquephenyl [●●●●●], some with extensive alkylation. Also of note are C<sub>8</sub>, C<sub>10</sub>, and C<sub>12</sub>-alkylbenzenes [Bx], C<sub>6</sub>-alkylstyrenes [St6], and alkylnaphthalenes [Nx]. Alkylated 2- to 5-ring polyphenyls with one or more oxygens and possibly nitrogen are tentatively identified in the resin fraction (Fig. 5C), which notably accounts for nearly half of the total solvent extract (Table S1).

In a simpler reflection of the aromatic fraction's image, the thermally desorbed polyphenyls range from the 2- to the 4-ring and are accompanied by long-chain alkylbenzenes (Fig. 5D). Interestingly, phenylnaphthalene isomers [PNAP] and simple monoaromatics including styrene and methylstyrene [St, St1] appear here, but not in the aromatic fraction. The thermodesorption residue yielded a simpler distribution of 2- to 5-ring polyphenyls upon pyrolysis, while the most important component is styrene, along with benzene, toluene, methylstyrene, phenylnaphthalene, and minor amounts of PAHs (Fig. 5E). The asphaltene pyrolyzate is similar but simpler yet, containing predominantly styrene and a few 2- to 4-ring polyphenyls (Fig. 5F).

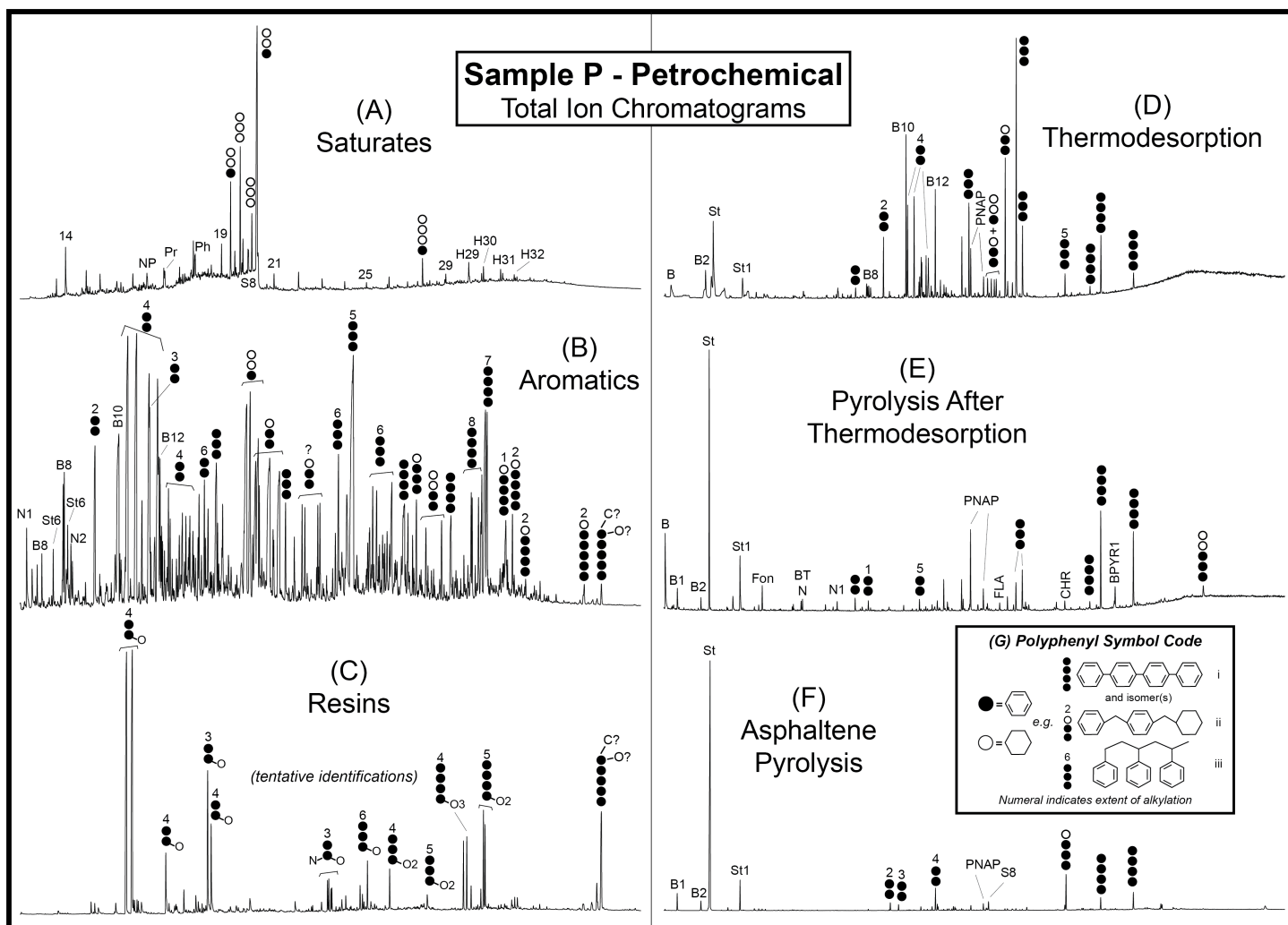


Figure 5. Total ion current chromatograms for petrochemical plant soil Sample P. (A) saturated hydrocarbons, (B) aromatics, (C) resins, (D) thermodesorption products, (E) products of sequential pyrolysis of the post-thermodesorption residue and (F) asphaltene pyrolysis products. See Table 1 for peak identification.

The former petrochemical plant at the site produced styrene using the styrene monomer propylene oxide (SMPO) process (Sec. 2.2.1), in which ethylbenzene and propylene react to produce styrene along with propylene oxide via several intermediates using catalysis (Buijink et al., 2008). Unfortunately, styrene oligomers and unspecified ethers accumulate in the reaction mixture as unwanted heavy by-products of the process and create a costly disposal problem for the operator (Buijink et al., 2008). The diverse polyphenyls apparent in Figure 5A-F are evidently a highly complex mixture of styrene oligomers, most likely representing SMPO process by-products that contaminated the soil during the course of plant operations (Table 2). There is relatively more styrene in the pyrolysis products likely due to high temperature cracking of the oligomers during the analysis (Fig. 5E, F). Isoprenoids and hopanes seen in the saturated fraction indicate that biodegraded petroleum products constitute a relatively minor additional contaminant. Recognition of the particular nature of the pollutants afflicting this brownfield site would lead to a more effective remedial plan of action.

### 3.2.5. Sample M - Metallurgical waste and soil

The saturated hydrocarbon fraction of metallurgical waste and soil Sample M (Fig. 6A) exhibits prominent isoprenoids [NP, Pr, Ph] and hopanes [Tm, Hn] above a very broad UCM hump that peaks beneath the C<sub>34</sub> hopanes [H34]. C<sub>14</sub>-C<sub>35</sub> *n*-alkanes are also present, with a pronounced long-chain odd carbon number preference. A few parent 3- and 4-ring PAHs [PHN, FLA, PYR, BAN, CHR] strongly predominate in the relatively simple distribution of aromatic hydrocarbons (Fig. 6B). *n*-Octadecanol [OL18] and *n*-docosenamide [AM22] are important components of the resin fraction, accompanied by other minor alkanols and alkylamides with even carbon number chains (Fig. 6C). The presence of plasticizers [X], sterols [STLn] and a terpenoid similar to  $\beta$ -amyrin [BAM] is also

noteworthy. Directly pyrolyzing the raw sample at 610 °C produced a simple, but highly unusual trace with only two important peaks identified (Fig. 6D). The largest corresponds to the arsenic oxide mineral arsenolite, while the smaller is attributed to metallic mercury. There are so significant organic compounds detected. The presence of arsenolite was confirmed by SEM and EDS (Fig. 6E, F). Although the solvent extract is mostly asphaltenes (85.5%, Table S1), asphaltene pyrolysis provided only limited insights due to excessive mass spectral noise. Elemental Hg (monitored using  $m/z$  200 and 202) is present throughout the entire GC run and likely contributed to the problem, impairing the MS detector. Toluene and styrene produced the sole recognizable peaks on the asphaltene pyrogram (not shown), although other hydrocarbons (*n*-alk-1-enes and PAHs) are evident in trace quantities. The presence of mercury will have inflated the measured mass of the asphaltene fraction, which therefore should be interpreted with caution. In this experiment, elemental Hg was unexpectedly introduced into the mass spectrometer, a practice that should be avoided to prevent undue impairment of the instrument.

## Figure 6

In the pyrometallurgical process formerly employed at the brownfield site, sulfide ores of mercury and arsenic (cinnabar, orpiment, realgar) were roasted in direct contact with petroleum-derived fuel oil in a kiln, with the oxide arsenolite being the main by-product as Hg was mostly recovered in the condensation systems (Gallego et al., 2015). The resulting waste thus contains both inorganic and organic components. Partially biodegraded fuel oil and combustion-derived parent PAHs imprint their signatures on the saturated and aromatic fractions, respectively (Table 2). While the alkanols and alkylamides might indicate biological input, contamination from cosmetics during sample handling cannot be excluded.

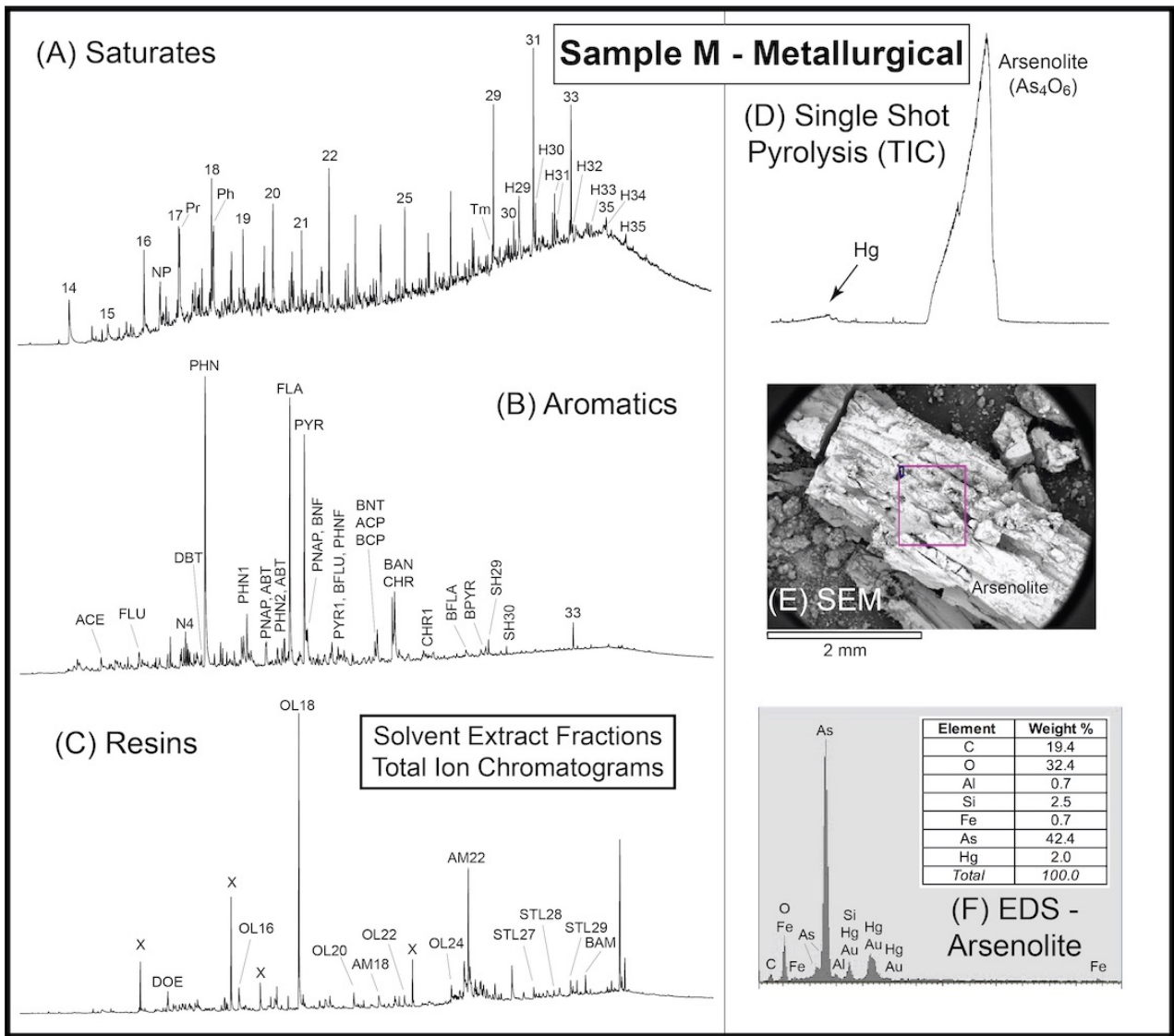


Figure 6. Total ion current chromatograms for metallurgical waste-contaminated soil Sample M. (A) saturated hydrocarbons, (B) aromatics, (C) resins, (D) combined thermodesorption and pyrolysis products produced in a single shot run at 610°C. See Table 1 for peak identification. (E) SEM micrograph of arsenolite crystals found in the samples. (F) EDS results from the arsenolite crystal imaged in E.

The odd carbon number alkanes in the saturated fraction and the sterols and terpenoid in the resins indicate additional input from the vegetation that colonized the site since its abandonment (Fernández et al., 2017). The pyrogram (Fig. 6D) is very unusual, but nevertheless shows that Py-GC-MS has the surprising ability to detect certain inorganic substances if they can be vaporized at the temperature employed.

#### 4. Conclusions

A comprehensive study of each sample has facilitated the acquisition of complementary information from the different analytical approaches in the previous sections (Table 2). In general terms, the fingerprints obtained are very similar when the main contaminants are oil products (Samples F and R), and therefore the non-extracting approach (no sample preparation, rapid and inexpensive) is favored. On the other hand, the main peaks and their abundances are usually different when studying complex residues (Samples C and P), and thus both approaches are complementary. In any case, however, pyrolytic techniques can be useful in identifying specific characteristics such as the presence of very heavy compounds (Sample C), mixed organic and inorganic compounds (Sample M), and oligomers (Sample P).

The environmental forensic studies of soils affected by multiple pollution sources are tedious, involve long periods of time for their analysis and require deep knowledge of the origin of different pollutants. In this work, a multifaceted environmental forensics approach revealed key molecular features of a diverse, genetically unrelated suite of industrial complexly-contaminated soils. This is shown to be particularly critical if the spill is an atypical industrial discharge, necessitating painstaking characterization of unfamiliar



substances lying outside of existing regulatory regimes and thus overlooked by mandated analytical protocols (i.e., contaminants of emerging concern).

Specifically, LC fractionation was revealed to be a very useful tool for separation of complex mixtures of legacy contaminants in order to perform full-scan GC-MS identifications, much more powerful for forensic purposes than usual quantitative techniques. In addition to the commonly employed GC-MS analysis of saturated and aromatic fractions, the investigation of the resin fractions provided important insights.

As a rapid alternative, TD-GC-MS combined with Py-GC-MS, which require only minimal sample preparation, was sufficient to identify the majority of the contaminants present at the sites, and therefore it proves to be very useful as a screening system to quickly obtain qualitative results in soil pollution studies. Specifically, desorption and pyrolytic techniques can accurately identify particular characteristics such as the presence of sulfur aromatics (sample F), complex mixtures of PAHs and biodegraded petroleum (Sample R), very heavy compounds (Sample C), mixed organic and inorganic compounds (Sample M) and oligomers (Sample P).

In summary, the rapid, inexpensive screening provided by TD- and/or Py-GC-MS would be advantageous to remediation practitioners when used for a "first look" at a brownfield site with unknown contaminants. It would be similarly beneficial for the detection of unusual or unexpected contaminants, including those currently outside of the regulatory framework. If needed, subsequent detailed quantitative analyses could be then be more effectively focused on the components detected in the screening. The screening could also guide decisions when choosing appropriate site remediation methods, e.g., to avoid attempting bioremediation of a spill that is already biodegraded. The comprehensive environmental forensic approach presented herein can serve to better inform the planning and regulation of brownfield remediation in the public interest.

## Acknowledgements

The authors would like to thank the Environmental Assays Unit of the Scientific and Technical Services (SCTs) of the University of Oviedo for its collaboration and technical support. We also like to thank Mercedes Díaz Somoano (INCAR-CSIC) for kindly providing us with the P sample.

## References

- Alimi, H., Ertel, T., Schug, B., 2003. Fingerprinting of hydrocarbon fuel contaminants: literature review. *Environ. Forensics* 4, 25-38. <https://doi.org/10.1080/15275920303489>.
- ASTM, 2007. Standard Test Method for *n*-Heptane Insolubles: Annual Book of the American Society For Testing Materials Standards, v. 05.01 and 05.02. ASTM International, West Conshohocken, PA, USA.
- Balseiro-Romero, M., Macías, F., Monterroso, C., 2016. Characterization and fingerprinting of soil and groundwater contamination sources around a fuel distribution station in Galicia (NW Spain). *Environ. Monit. Assess.* 188, 292. <https://doi.org/10.1007/s10661-016-5288-1>.
- Bari, M.A., Baumbach, G., Kuch, B., Scheffknecht, G., 2009. Wood smoke as a source of particle-phase organic compounds in residential areas. *Atmos. Environ.* 43, 4722-4732. <https://doi.org/10.1016/j.atmosenv.2008.09.006>.
- Boehm, P.D., Douglas, G.S., A. Burns, W.A., Mankiewicz, P.J., Page, D.S., Bence, A.E., 1997. Application of petroleum hydrocarbon chemical fingerprinting and allocation techniques after the Exxon Valdez oil spill. *Mar. Pollut. Bull.* 34, 599-613. [https://doi.org/10.1016/S0025-326X\(97\)00051-9](https://doi.org/10.1016/S0025-326X(97)00051-9).

- Bopp, R.F., Simpson, H.J., Olsen, C.R., Kostyk, N., 1981. Polychlorinated biphenyls in sediments of the tidal Hudson River, New York. *Environ. Sci. Technol.*, 15, 210-216. <https://doi.org/10.1021/es00084a007>.
- Buijink, J.K.F., Lange, J.-P., Bos, A.N.R., Horton, A.D., Niele, F.G.M., 2008. Propylene epoxidation via Shell's SMPO process: 30 years of research and operation, in: Oyama, S.T. (Ed.) *Mechanisms in Homogeneous and Heterogeneous Epoxidation Catalysis*, Elsevier, pp. 355-371. <https://doi.org/10.1016/B978-0-444-53188-9.00013-4>.
- Bujalski, N.M., 2010. Characterization of contaminant and biomass-derived organic matter in sediments from the Lower Passaic River, New Jersey, USA. MS Thesis. Montclair State University, Montclair (NJ), 110 p.
- de la Cruz, C., Márquez, N., Escobar, M., Segovia, S., 1997. An improved chromatographic method for the separation of saturated hydrocarbons, aromatic hydrocarbons, resins and asphaltenes from heavy crude oils, in: *Preprints of Papers Presented at the 213th American Chemical Society National Meeting*. San Francisco, p. 416–8.
- Douglas, G.S., Emsbo-Mattingly, S.D., Stout, S.A., Uhler, A.D., McCarthy, K.J., 2007. Chemical fingerprinting methods, in: Murphy, B. L., Morrison, R.D. (Eds.), *Introduction to Environmental Forensics*. Elsevier Academic Press, London, pp. 311-454. <https://doi.org/10.1016/B978-012369522-2/50010-5>.
- Emsbo-Mattingly, S.D., Stout, S.A., 2011. Semivolatile residues of coal and coal tar, in: Stracher, G.B., Prakash, A., Sokol, E.V. (Eds.), *Coal and Peat Fires: A Global Perspective*. Elsevier, pp. 173-208. <https://doi.org/10.1016/B978-0-444-52858-2.00011-6>.
- Fernández, S., Poschenrieder, C., Marcenò, C., Gallego, J. R., Jiménez-Gámez, D., Bueno, A., Afif, E., 2017. Phytoremediation capability of native plant species living on Pb-Zn and Hg-As mining wastes in the Cantabrian range, north of Spain. *J. Geochem. Explor.*, 174, 10-20. <https://doi.org/10.1016/j.gexplo.2016.05.015>.

- Gallego, J. R., Esquinas, N., Rodríguez-Valdés, E., Menéndez-Aguado, J. M., & Sierra, C. (2015). Comprehensive waste characterization and organic pollution co-occurrence in a Hg and As mining and metallurgy brownfield. *J. Hazard. Mater.*, 300, 561-571. <https://doi.org/10.1016/j.jhazmat.2015.07.029>.
- García, R., Díaz-Somoano, M., Calvo, M., López-Antón, M.A., Suárez, S., Suárez Ruiz, I., Martínez-Tarazona, M.R., 2012. Impact of a semi-industrial coke processing plant in the surrounding surface soil. part II: PAH content. *Fuel Process. Technol.*, 104, 245-252. <https://doi.org/10.1016/j.fuproc.2012.05.018>.
- González-Fernández, B., Rodríguez-Valdés, E., Boente, C., Menéndez-Casares, E., Fernández-Braña, A., Gallego, J.R., 2018. Long-term ongoing impact of arsenic contamination on the environmental compartments of a former mining-metallurgy area. *Sci. Total. Environ.*, 610-611, 820-830. <https://doi.org/10.1016/j.scitotenv.2017.08.135>.
- Grimalt, J.O., Fernández, P. Bayona, J.M., Albaigés, J., 1990. Assessment of fecal sterols and ketones as indicators of urban sewage inputs to coastal waters. *Environ. Sci. Technol.*, 24, 357-363. <https://doi.org/10.1021/es00073a011>.
- Hagmann D.F., Kruger M.A., Cheung M., Mastalerz M., Gallego J.L.R., Singh J.P., Krumins J.A., Li X., Goodey N., 2019. Environmental forensic characterization of former rail yard soils located adjacent to the Statue of Liberty in the New York/New Jersey harbor. *Sci. Total Environ.* 690,1019-1034. <https://doi.org/10.1016/j.scitotenv.2019.06.495>.
- Hatcher, P.G., Faulon, J.L., Wenzel, K.A., Cody, G.D., 1992. A structural model for lignin-derived vitrinite from high-volatile bituminous coal (coalified wood). *Energ. Fuel* 6, 813-820. <https://doi.org/10.1021/ef00036a018>.
- Huntley, S.L., Iannuzzi, T.J., Avantaggio, J.D., Carson-Lynch, H., Schmidt, C.W., Finley, B.L., 1997. Combined sewer overflows (CSOs) as sources of sediment contamination in the lower Passaic River, New Jersey. II. Polychlorinated dibenzo-p-dioxins,

- polychlorinated dibenzofurans, and polychlorinated biphenyls. *Chemosphere* 34, 233–250.  
[https://doi.org/10.1016/S0045-6535\(96\)00374-8](https://doi.org/10.1016/S0045-6535(96)00374-8).
- Iannuzzi, T.J., Huntley, S.L., Bonnevie, N.L., Finley, B.L., Wenning, R.J., 1995. Distribution and possible sources of polychlorinated biphenyls in dated sediments from the Newark Bay estuary, New Jersey. *Arch. Environ. Con. Tox.*, 28, 108-117.  
<https://doi.org/10.1007/BF00213975>.
- Iannuzzi, T.J., Huntley, S.L., Schmidt, C.W., Finley, B.L., McNutt, R.P., Burton, S.J., 1997. Combined sewer overflows (CSOs) as sources of sediment contamination in the lower Passaic River, New Jersey. I. Priority pollutants and inorganic chemicals, *Chemosphere*, 34, 213-231. [https://doi.org/10.1016/S0045-6535\(96\)00373-6](https://doi.org/10.1016/S0045-6535(96)00373-6).
- Isobe, K.O., Tarao, M., Zakaria, M.P., Chiem, N.H., Minh, L.Y., Takada, H., 2002. Quantitative application of fecal sterols using gas chromatography-mass spectrometry to investigate fecal pollution in tropical waters: Western Malaysia and Mekong Delta, Vietnam, *Environ. Sci. Technol.*, 36, 4497-4507. <https://doi.org/10.1021/es020556h>.
- Jewell, D.M, Albaugh, E.W., Davis, B.E., Ruberto, R.G., 1974. Integration of chromatographic and spectroscopic techniques for the characterization of residual oils. *Ind. Eng. Chem. Fundamen.*, 1974, 13, 278-282. <https://doi.org/10.1021/i160051a022>
- Kruege M.A., 2015. Analytical pyrolysis principles and applications to environmental science, in, M. Barbooti, ed., *Environmental Applications of Instrumental Chemical Analysis*. CRC Press, Boca Raton (FL), p. 533-569. <https://doi.org/10.1201/b18376>.
- Kruege, M.A., Bensley, D.F., 1994. Flash pyrolysis-gas chromatography/mass spectrometry of Lower Kittanning vitrinites: Changes in the distributions of polyaromatic hydrocarbons as a function of coal rank, in: Mukhophadyay, P. K., Dow, W.G. (Eds.), *Vitrinite Reflectance as a Maturity Parameter: Applications and Limitations*. ACS Symposium Series 570, pp. 136-148. <https://doi.org/10.1021/bk-1994-0570.ch009>.

- Kruege, M.A., Permanyer, A., 2004. Application of pyrolysis-GC/MS for rapid assessment of organic contamination in sediments from Barcelona harbor. *Org. Geochem.* 35, 1395-1408. <https://doi.org/10.1016/j.orggeochem.2004.05.008>.
- Kruege, M.A., Permanyer, A., Serra, J., Yu, D., 2010. Geochemical investigation of an offshore sewage sludge deposit, Barcelona, Catalonia, Spain. *J. Anal. Appl. Pyrol.*, 89, 204-217. <https://doi.org/10.1016/j.jaap.2010.08.005>.
- Kruege, M.A., Gallego, J.R., Lara-Gonzalo, A., Esquinas, N., 2018. Environmental forensics study of crude oil and petroleum product spills in coastal and oilfield settings: Combined insights from conventional GC-MS, thermodesorption-GC-MS and pyrolysis-GC-MS, in: Stout, S.A., Wang, Z. (Eds.), *Oil Spill Environmental Forensics Case Studies*. Butterworth-Heinemann (Elsevier), United States/United Kingdom, pp. 131-155. <https://doi.org/10.1016/B978-0-12-804434-6.00007-0>.
- Lara-Gonzalo, A., Kruege, M.A., Lores, I., Gutiérrez, B., Gallego, J.R., 2015. Pyrolysis GC-MS for the rapid environmental forensic screening of contaminated brownfield soil. *Org. Geochem.*, 87, 9-20. <https://doi.org/10.1016/j.orggeochem.2015.06.012>.
- Laumann, S., Micić, V., Kruege, M.A., Achten, C., Sachsenhofer, R.F., Schwarzbauer, J., Hofmann, T., 2011. Variations in concentrations and compositions of polycyclic aromatic hydrocarbons (PAHs) in coals related to the coal rank and origin. *Environ. Pollut.*, 159, 2690-2697. <https://doi.org/10.1016/j.envpol.2011.05.032>.
- Malcolm Pirnie, Inc., 2006. Lower Passaic River Restoration Project Draft Geochemical Evaluation (Step 2). Prepared for US Environmental Protection Agency Region 2 and US Army Corps of Engineers Kansas City District. Version 2006/03/06. 421 p. Accessed 2019/07/17. [http://passaic.sharepointspace.com/Public Documents/2006-03-06 Draft Geochemical Evaluation \(Step 2\) MPI.pdf](http://passaic.sharepointspace.com/Public Documents/2006-03-06 Draft Geochemical Evaluation (Step 2) MPI.pdf)

- Medeiros P.M., Simoneit, B.R.T., 2007. Gas chromatography coupled to mass spectrometry for analyses of organic compounds and biomarkers as tracers for geological, environmental, and forensic research. *J. Sep. Sci.*, 30, 1516-1536.  
<https://doi.org/10.1002/jssc.200600399>.
- Mudge, S.M., Bebianno, M.J., 1997. Sewage contamination following an accidental spillage in the Ria Formosa, Portugal, *Mar. Pollut. Bull.*, 34, 163-170.  
[https://doi.org/10.1016/S0025-326X\(96\)00082-3](https://doi.org/10.1016/S0025-326X(96)00082-3).
- Nishioka, M., Chang, H.C., Lee, M.L., 1986. Structural characteristics of polycyclic aromatic hydrocarbon isomers in coal tars and combustion products, *Environ. Sci. Technol.*, 20, 1023-1027. <https://doi.org/10.1021/es00152a010>.
- Peters, K.E., Walters, C.C., Moldowan, J.M., 2005. *The Biomarker Guide. Vol. 2. Biomarkers and Isotopes in Petroleum Exploration and Earth History*, Cambridge University Press, Cambridge, 1155 p.
- Quadrini, J. D., Ku, W., Connolly, J. P., Chiavelli, D. A., & Israelsson, P. H., 2015. Fingerprinting 2,3,7,8-tetrachlorodibenzodioxin contamination within the lower Passaic River. *Environ. Toxicol. Chem.*, 34, 1485-1498. <https://doi.org/10.1002/etc.2961>.
- Ramdahl, T., 1983. Retene - a molecular marker of wood combustion in ambient air. *Nature* 306, 580-582. <https://doi.org/10.1038/306580a0>.
- Rosell-Melé, A., Moraleda-Cibrián, N., Cartró-Sabaté, M., Colomer-Ventura, F., Mayor, P., Orta-Martínez, M., 2018. Oil pollution in soils and sediments from the Northern Peruvian Amazon. *Sci. Total Environ.*, 610-611, 1010-1019.  
<https://doi.org/10.1016/j.scitotenv.2017.07.208>.
- Schobert, H.H., Song, C., 2002. Chemicals and materials from coal in the 21st century. *Fuel* 81, 15-32. [https://doi.org/10.1016/S0016-2361\(00\)00203-9](https://doi.org/10.1016/S0016-2361(00)00203-9).

- Simoneit, B.R.T., 2002. Biomass burning - review of organic tracers for smoke from incomplete combustion. *Appl. Geochem.*, 17, 129-16. [https://doi.org/10.1016/S0883-2927\(01\)00061-0](https://doi.org/10.1016/S0883-2927(01)00061-0).
- Stankiewicz, B. A., Kruge M. A., Crelling, J. C., 1994a. Geochemical characterization of maceral concentrates from Herrin No. 6 coal (Illinois Basin) and Lower Toarcian shale kerogen (Paris Basin), in: Curnelle, R., Sévérac, J.-P. (Eds.), *Pétrologie Organique, Recueil des Communications, Colloque International des Pétrographes Organiciens Francophones, Bulletin des Centres de Recherches Exploration-Production Elf-Aquitaine*, Vol. 18, p. 237-251.
- Stankiewicz B.A., Kruge M.A., Crelling J.C., Salmon G.L., 1994b. Density gradient centrifugation: application to the separation of macerals of Type I, II and III sedimentary organic matter. *Energ. Fuel* 8,1513-1521. <https://doi.org/10.1021/ef00048a042>.
- Stout, S.A., Litman, E., Baker, G., Franks, J.S., 2018. Novel biological exposures following the *Deepwater Horizon* oil spill revealed by chemical fingerprinting, in: Stout, S.A., Wang, Z. (Eds.), *Oil Spill Environmental Forensics Case Studies*. Butterworth-Heinemann (Elsevier), United States/United Kingdom, pp. 757-784. <https://doi.org/10.1016/B978-0-12-804434-6.00033-1>.
- Thavamani, P., Mallapar, M., Krishnamurti, G.S.R., McFarland, R., Naidu, R., 2011. Fingerprinting of mixed contaminants from former manufactured gas plant (MGP) site soils: Implications to bioremediation. *Environ. Int.*, 37, 184-189. <https://doi.org/10.1016/j.envint.2010.08.017>.
- Tissot, B.P., Welte, D.H., 1984. *Petroleum Formation and Occurrence*. Springer, 702 p.
- Uhler, A.D., Emsbo-Mattingly, S.D., 2006. Environmental stability of PAH source indices in pyrogenic tars. *B. Environ. Contam. Tox.*, 76:689-696. <https://doi.org/10.1007/s00128-006-0975-1>.



- Uhler, A.D., Stout, S.A., Emsbo-Mattingly, S.D., Rouhani, S., 2010. Chemical fingerprinting: Streamlining site assessment during the sustainable redevelopment process, in: Brown, K., Hall, W.L., Snook, M., Garvin, K. (Eds.), *Sustainable Land Development and Restoration: Decision Consequence Analysis*. Elsevier, United States, pp. 325-343.  
<https://doi.org/10.1016/B978-1-85617-797-9.00016-2>.
- USEPA, 1996. SW-846 Test Method 3630C: Silica Gel Cleanup. Rev. 3. United States Environmental Protection Agency. <https://www.epa.gov/hw-sw846/sw-846-test-method-3630c-silica-gel-cleanup>.
- USEPA, 2019. Superfund Site: Diamond Alkali Co., Newark, NJ, Cleanup Activities. United States Environmental Protection Agency. Accessed 2019/07/17.  
<https://cumulis.epa.gov/supercpad/SiteProfiles/index.cfm?fuseaction=second.cleanup&id=0200613>
- USEPA-USACE, 2019. Passaic River Public Digital Library: Passaic River Datasets. United States Environmental Protection Agency and United States Army Corps of Engineers. Accessed 2019/07/16. [http://passaic.sharepointspace.com/SitePages/Passaic River Datasets.aspx](http://passaic.sharepointspace.com/SitePages/Passaic%20River%20Datasets.aspx)
- Wait, D., Ramsey, C., 2007. The measurement process. In: Murphy, B.L., Morrison, R.D. (Eds.), *Introduction to Environmental Forensics*. Elsevier Academic Press, London, pp. 83-128. <https://doi.org/10.1016/B978-012369522-2/50005-1>.
- Yunker, M.B., Macdonald, R.W., Vingarzan, R., Mitchell, R.H., Goyette, D., Sylvestre, S., 2002. PAHs in the Fraser River basin: a critical appraisal of PAH ratios as indicators of PAH source and composition, *Org. Geochem.* 33: 489-515.  
[https://doi.org/10.1016/S0146-6380\(02\)00002-5](https://doi.org/10.1016/S0146-6380(02)00002-5).

## Supplementary Material

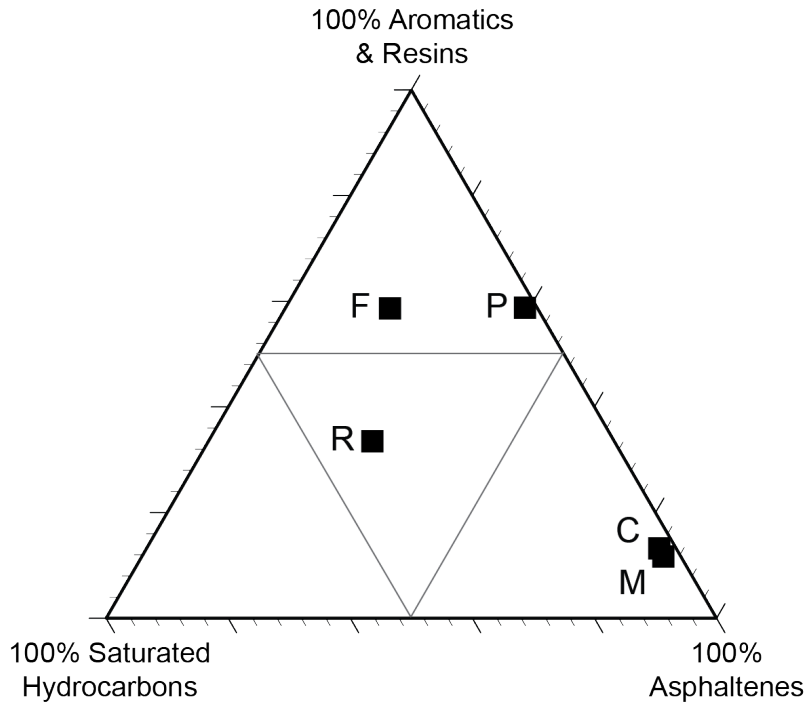


Figure S1. Ternary diagram showing bulk compositions as determined by deasphalting and liquid chromatography (Fig. 1, Table 1).

Sample	Type	TSE (g/kg dry soil)	Saturates (LC fractions as weight percent of total extract)	Aromatics	Resins	Asphaltenes
F	fuel spill	NA	24.3	36.7	21.7	17.3
C	coke oven	9.32	2.9	3.6	9.4	84.1
R	urban river	8.46	39.8	15.6	17.7	26.9
P	petrochemical	9.33	2.2	11.0	47.5	39.3
M	metallurgical	5.06	3.1	1.5	9.9	85.5

Table S1. Bulk composition of the samples studied.